NBSIR 75-805

CALIBRATION TECHNIQUES FOR ELECTROMAGNETIC HAZARD METERS: 500 MHz to 20 GHz
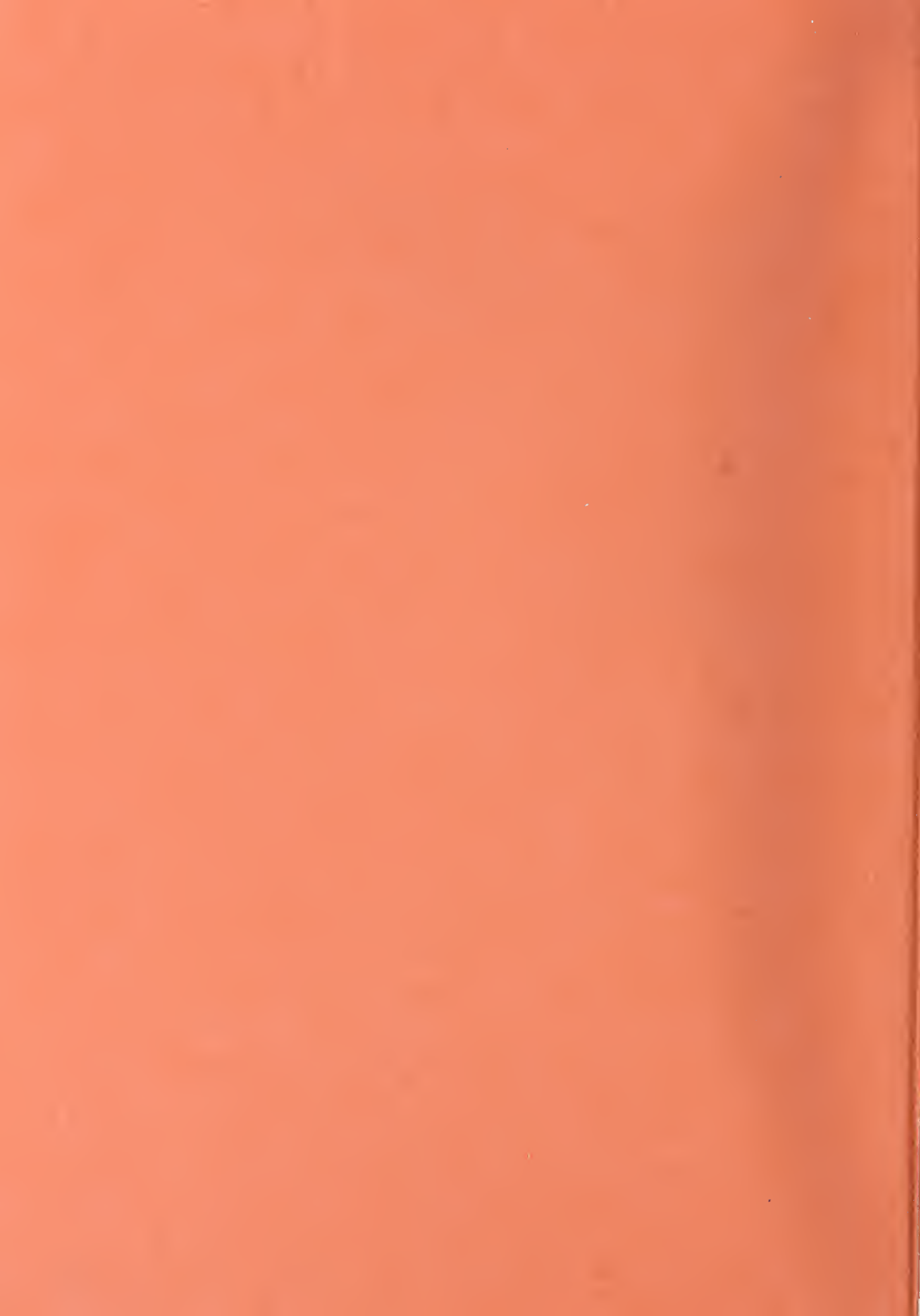
Ronald R. Bowman

Electromagnetics Division
Institute for Basic Standards
National Bureau of Standards
Boulder, Colorado   80302

April   1976

NBSIR 75-805

CALIBRATION TECHNIQUES FOR ELECTROMAGNETIC HAZARD METERS: 500 MHz to 20 GHz

Ronald R. Bowman

Electromagnetics Division
Institute for Basic Standards
National Bureau of Standards
Boulder, Colorado 80302

April 1976

CONTENTS

LIST OF TABLES

LIST OF FIGURES

CALIBRATION TECHNIQUES FOR ELECTROMAGNETIC HAZARD METERS: 500 MHz TO 20 GHz

Ronald R. Bowman

ABSTRACT

The calibration techniques discussed are suitable for producing fields for calibrating most electromagnetic (EM) hazard meters to within ± 1.0 dB using a minimum of laboratory space and oscillator power. Above about 2.6 GHz, adequate equipment and standards have been available for these calibrations. Below this frequency the large apertures of the usual horn radiators require more power than is available from medium power oscillators. Further, calibrations in closed systems are difficult except at frequencies well below 1 GHz. Thus there is a need for small-aperture gain standards from about 500 MHz to 2.6 GHz. The main portion of the work reported here consists of accurate gain measurements for open-ended hollow waveguide radiators (OEG) for use from 500 MHz to 2.6 GHz. Other characteristics of this type of radiator important for EM hazard meter calibrations were also determined: near-field corrections, reflection coefficients, and aperture scattering. The suitability of the calibration scheme was tested by performing calibrations at 2 GHz on an EM hazard meter with both a horn radiator and an OEG radiator.

Key words: Calibrations; electromagnetic hazards; field meters; gain; microwave; near-field.

1.   INTRODUCTION

This report describes work performed to provide improved capability for calibrating electromagnetic hazard meters in the frequency range from, primarily, 500 MHz to 2.6 GHz. The emphasis is on calibrations of moderate accuracy with a minimum of laboratory space and oscillator power required. The calibration techniques described are also suitable for performing calibrations up to 20 GHz and beyond. The work was sponsored by the Calibration Coordination Group of the Department of Defense.

1.1 Objectives

The contractual objectives of the effort were to determine satisfactory techniques for calibrating electromagnetic (EM) hazard meters to within ± 1.0 dB from 0.9 GHz (or lower) to 20 GHz (or higher) and to perform the necessary work to implement these techniques. Because of limited funding, it was necessary to carefully restrict the work to the most important essentials, as discussed in section 2. The calibration techniques are also useful below 0.9 GHz, but their implementation requires increasing anechoic chamber size and oscillator power with decreasing frequency.

1.2 Orientation

The objectives of this effort are to be accomplished within several con-
straints. The calibration scheme is to use only commercially available
equipment, allow calibration at 10 mW/cm^2 or higher field levels (above
0.9 GHz), use a small amount of space, and require only moderate-power oscil-
lators (see section 2.4).

An important consequence of these restrictions is that the volume of
the calibration field will be necessarily small. For all existing EM hazard
meters, this means that only the field sensor of the meter can be placed in
the region of (approximately) uniform calibration field and that the other
parts of the meter may be subjected to much lower field levels. Thus, for
example, an interaction between the field sensor and the case of the instru-
ment may be quite different in the calibration situation than in a true far-
field plane-wave situation. The effects of the operator and case will usually
have to be determined using larger spaces and source powers of 100 watts or
more. In using the meter, these effects may or may not be important depending
on the instrument design, the field being measured, and the method of opera-
tion of the meter. The associated perturbations of the meter reading may
well be more than the desired uncertainty limits of ± 1 dB, particularly
for the newer instrument designs that usually have omnidirectional or nearly
isotropic response. Because these effects are so variable, it is considered
desirable to minimize them while performing calibrations of the field sensor.
The scheme described here helps to provide this minimization.

1.3 Calibration Methods Considered

Due to limited funding, only established calibration methods were practi-
cal to implement. The proximity correction method* (see section 2.2) developed
earlier [1,2] for calibrating field intensity meters and EM hazard meters is
basically satisfactory, but some further work was necessary to implement
this method for use below 2.6 GHz. This method, as further developed, has the
following important features: (a) it requires much less oscillator power
than when using large antenna separations; (b) the calibration techniques
are suitable for small indoor antenna ranges; and (c) the techniques are
simple, involve basically the same procedure throughout the frequency range
of interest, and employ only commercially available equipment.

---

*The term "proximity correction" as used here and in [3,4] is identical to the
 term "near-zone correction" as used in [1,2]. "Proximity" has been used
 more often in the open literature than "near-zone," and the author prefers
 the former expression. These expressions have been defined to emphasize that
 both the receiving antenna and the transmitting antenna determine in an
 inseparable way the power transfer between antennas that are "proximate."
 In contrast, the term "near-field" is usually defined [5,p. 189;6;7] with
 respect to a single transmitting antenna and is not strictly relevant for
 real measurement situations where a receiving antenna or probe is always
 present.

Some attention was given to two other alternatives:

(1) A closed system (for example, a hollow waveguide or a "TEM cell" [8] terminated in either a short or a matched load) can be used to establish accurately known fields. Under certain conditions probes and instruments can be introduced into such a closed system and accurately calibrated. This method is attractive because it requires a minimum of oscillator power and laboratory space. However, this method is not suitable for the frequency range of interest because only a few commercially available EM hazard meters are capable of being calibrated by this method except at frequencies much below 0.9 GHz (primarily because they have field probes that are too large to be introduced into closed systems without seriously perturbing the known field). For a discussion of the use of this method for frequencies much below 0.9 GHz, see [8].

(2) It appears feasible to develop stable, isotropic field sensors for use as calibrated standards at frequencies at least as high as 10 GHz. Probably, only one field probe would be required to cover the range from 10 MHz to 10 GHz. Using this method, EM hazard meters would be calibrated simply by comparing them in the same fields (either in open space or in closed systems) with a stable laboratory-quality field meter. This method could not be implemented because the development cost is too great at the present time; but, eventually, it may provide the simplest and cheapest calibration scheme over a large frequency range [9].

2. PROBLEM DEFINITION

2.1 Introduction

A significant part of the work described here was to clearly determine the further work necessary to establish ± 1.0 dB calibration capability over at least the frequency range 0.9 to 20 GHz. By carefully restricting the work to the most essential needs, it was possible to provide an expanded data base so that reasonably satisfactory calibrations can be performed with available equipment from about 0.5 MHz to over 20 GHz. The following analysis of the calibration problem is important for understanding the present work as well as for indicating some remaining weaknesses in the present calibration methods for EM hazard meters.

2.2 The Proximity Correction Method: Some Relevant Discussion

The proximity (or "near-zone") correction method developed earlier [1,2] for calibrating field strength meters and EM hazard meters has proven quite satisfactory. This method is currently used by the National Bureau of Standards and is fairly widely used elsewhere. The method uses the same

3

procedures that would be used for large separations except that small separations are used and a correction is employed to remove the associated error. Given the necessary corrections, the proximity correction method avoids the serious difficulties (large multipath interference and much greater source power) involved with large separation distances. Advanced techniques are available [4] for measuring proximity corrections without using large separation distances. Though the measurement of these corrections is sometimes difficult, the effort is justified if more than a few probes or antennas of a given type are to be eventually calibrated. Except for a few subtle and troublesome details that are discussed below, the application of the proximity correction method is simple.

The calibrations under discussion here are for the response of the field sensor in a plane-wave field of power density S. If large separation distances d are used, S can be established with a known antenna of gain G by the basic formula

$$S = \frac{GP}{4\pi d^2} \qquad (d \rightarrow \infty) \qquad (2.1)$$

where P is the net power delivered to the antenna. (It is assumed throughout that the field point is on the axis of the transmitting antenna so that "G" means the maximum power gain.) Then if R is the reading of the meter, the calibration can be thought of as determining the calibration constant K by

$$K \equiv \frac{S}{R} = \frac{GP}{4\pi d^2 R} \qquad (d \rightarrow \infty). \qquad (2.2)$$

If short separation distances are used and C is the proper proximity correction, K is determined by

$$K = \frac{S}{CR} = \frac{GP}{4\pi d^2 CR} \qquad (2.3)$$

where S is calculated from eq. (2.1) despite small d. Note that eq. (2.2) is inherently approximate since it holds only asymptotically; but eq. (2.3) is exact insofar as all of the quantities are known. C is determined by the characteristics of the receiving antenna or sensor as well as the characteristics of the transmitting antenna. Further, C cannot be factored into two functions, one dependent only on the characteristics of the receiving antenna or probe and the other dependent only on the characteristics of the transmitting antenna [10]. Logically, therefore, C should be thought of as an overall correction applied to the response or reading R.

4

It is tempting (particularly when the field sensor is small) to identify
G/C as the "near-field gain"* of the transmitting antenna and S/C as the
actual near-field power density. However, for real situations this identifi-
cation can be correct only in an approximate sense and can be significantly
in error even when the receiving antenna or probe is small. For all existing
probes and antennas, the measurement of power density is dependent, implicitly,
on the known plane-wave relations between the electric and magnetic fields.
Strictly speaking, Maxwell's equations require that a plane-wave must be
infinite in extent and have uniform power density. For practical purposes it
is only necessary that the field in the vicinity of the probe or receiving
antenna, i.e., the "local" field, not differ significantly from the "true"
plane-wave configuration. In a plane-wave, the electric and magnetic vectors
are orthogonal to each other and to the propagation direction. Further, their
electrical phase differs by 180 degrees and their ratio is $(\mu_o/\varepsilon_o)^{\frac{1}{2}}$. If a
probe is located close to a radiator, one or more of these conditions can be
violated to a significant degree even if the local field is uniform in con-
figuration. Though it may be possible to build a probe that would measure
$S \equiv |\underline{E} \underline{H}^*|$ for any field configuration, no existing probes can do this. An
accurate proximity correction includes the difference in the probe response due
to any significant differences between the far-field and near-field configura-
tions. Though there is little direct evidence at present to substantiate the
claim, it is very unlikely that, for the on-axis separations discussed in this
report, the near-field configuration differs significantly from the far-field
configuration. (By "significant" it is meant in this discussion that the
associated error in a given measurement is more than 0.03 dB.) Insofar as
this claim is true, the proximity corrections for all small probes will be the
same for a given radiator and G/C will be essentially the near-field gain of
the radiator.

Except for the objections raised in the last paragraph, the "near-field
gain" concept is useful (and will be used in this report). Often G/C will be
nearly equal to the near-field gain of the transmitting antenna. When the
field sensor or receiving antenna is small with respect to the local field
variations and has the same response coefficient for the near-field power
density as for the far-field power density, the ratio of the far-field gain
to the near-field gain is the proper proximity correction. For such cases,
it is easy to determine proximity corrections for many antennas by using near-
field gain calculations as given, for example, in [6]. However, it is difficult

---

*The reader is cautioned that several definitions for near-field gain have
appeared in the literature, usually in an implicit way. Further, some of
these definitions are not physically very meaningful. As used here, "near-
field gain"is defined by eq. (2.1) except that d is finite and S is the power
density at the near-field point. (Some near-field definitions are for the
electric field strength or intensity rather than for S.)

to estimate the errors associated with these calculations as well as the errors associated with the above assumptions about the receiving system. Therefore, it is considered preferable to use measured proximity corrections even when calculated corrections are feasible.

It is important that eq. (2.3) not be misused by utilizing separations that are too small. If d is too small, the proximity corrections may have a significant dependence on the angular orientation of the field sensor at the field point (a serious complication only if the rotational response of the sensor is to be determined as part of the calibration). Also, for some types of EM hazard meters, the corrections may be a function of field intensity level as well. This last statement may seem surprising; but it follows simply from the fact that, unlike most antenna-receiver systems, some EM hazard probes have energy detectors spread out over a fairly large region. For example, a popular probe utilizes a series of thin-film thermocouples distributed on lossy strips extending about two to three centimeters. Under extreme near-field conditions, the field may not be uniform over the dimensions of the field sensor so that the thermocouples may have a different temperature configuration than they would have for a locally uniform field. The resulting error depends on, among other things, the linear dynamic range of the thermocouple detectors and could perhaps be significant under extreme near-field conditions. Obviously, the problems discussed in this paragraph need to be investigated. In the meantime, it is recommended that the near-zone correction method not be used for separations less than roughly a^2/λ where a is the diameter of a circular aperture, the side of a square aperture, or the larger side of a rectangular aperture. This criterion may well be too conservative, particularly for some antenna-probe situations, but the use of distances much smaller than a^2/λ should be accompanied by justification.

2.3 The Importance of Antenna Aperture Size for Electromagnetic Hazard Meter Calibrations

From eq. (2.3)

$$\frac{KR}{P} = \frac{G}{4\pi d^2 C} \qquad (2.4)$$

where KR/P is the "apparent" (as read by the meter) power density* per watt of net power delivered to the antenna. From the fundamental relation

$$G = \frac{4\pi A}{\lambda^2} , \qquad (2.5)$$

---

*Insofar as G/C is equal to the near-field gain, KR = S/C is equal to the true near-field power density. However, it is immaterial to the discussion in this section whether or not KR is the true near-field power density.

eq. (2.4) becomes

$$\frac{KR}{P} = \frac{A}{\lambda^2 d^2 C} \tag{2.6}$$

where A is the effective receiving area of the antenna. Expressing the separation distance in terms of the usual "normalizing" factor a^2/λ,

$$\frac{KR}{P} = \frac{A}{r^2 a^4 C}, \tag{2.7}$$

where a is the largest dimension of the aperture and $r = d(a^2/\lambda)^{-1}$. Assuming a rectangular aperture of dimensions a and b and using the aperture efficiency $\eta \equiv A/A_p$ where $A_p = ab$ is the physical aperture area, eq. (2.7) becomes

$$\frac{KR}{P} = \left(\frac{b}{a}\right)^2 \frac{\eta}{r^2 C A_p}. \tag{2.8}$$

Insofar as the quantities in eq. (2.8) are known, it is an exact relation. Some rather crude approximations and assumptions will now be introduced to provide a simple interpretation of eq. (2.8) and to estimate the approximate oscillator power required to establish a given apparent power density in terms only of the physical aperture area.

Except for apertures with one or more dimensions of about a wavelength or less, antennas with the same configuration of aperture illumination tend to have roughly the same aperture efficiency regardless of the aperture size. Further, for a given value of r and for small anechoic chambers, the uncertainties in the power density due to multipath interference and also to the proximity correction tend to be independent of aperture size. As a result, the process of "trading off" the uncertainties due to MPI, which tend to increase with r, and the uncertainties due to C, which tend to decrease with increasing r, usually leads to values of r roughly between 1 and 1.5. Thus, all of the variables on the right of eq. (2.8) except A_p are roughly constant for most situations. Then, the apparent power density obtainable per watt for a given measurement accuracy is inversely proportional to the physical aperture area of the antenna.

From eq. (2.8),

$$P = \left(\frac{a}{b}\right)^2 \frac{r^2 C A_p}{\eta} (KR). \tag{2.9}$$

For a typical horn antenna, an aperture efficiency of about 0.5 or more can be assumed; and an a/b ratio of 3/2 or less is a reasonable assumption. If near-field distances of r = 1 are used, C will usually be about 4/3 or less. Then for the usual commercial horn antennas,

$$P < 6 A_p(KR) \tag{2.10}$$

7

Comparing the predictions of eq. (2.10) with more detailed calculations for several horns suggests that eq. (2.10) is fairly conservative. Therefore, it is believed that eq. (2.11) is justified for likely designs for pyramidal horn antennas:

$$P < 5 \; A_p(KR) \qquad\qquad (2.11)$$

One more consideration is important in arriving at another useful estimation formula. While calibrating EM hazard meters, it is convenient to use a fixed separation distance for all frequencies within the operating band of the antenna. If a fixed separation is chosen so that $r = 1$ for the highest frequency in the band, r will be about 1.5 for the lowest frequency in the usual operating band for horns. If the same procedure used to derive eq. (2.11) is repeated, and estimating that C will be typically less than 1.15 for separations of $r = 1.5$, it follows that

$$P_M < 10 \; A_p(KR) \qquad\qquad (2.12)$$

where P_M is an estimate of the maximum required power at the low end of (and, therefore, throughout) the operating band for a distance where $r = 1$ at the high end of the band.

Though eqs. (2.11) and (2.12) are approximate, they are useful for rough estimates. The major inaccuracy in these formulas is that they over estimate the required power for horns with small flare angles (because such horns have much higher aperture efficiencies than 0.5 and also have relatively small proximity corrections). Also, apertures that have one or more dimensions of about one wavelength or less are apt to have relatively high aperture efficiencies. For small aperture horns with small flare angles, and particularly for open-ended guides, eqs. (2.11) and (2.12) can over estimate the required power by a factor of two or more.

The advantages of using a small aperture to minimize the required oscillator power is particularly pronounced for the case of horn radiators. If the flare length of a horn is kept fixed while the aperture area is reduced, the rather large aperture "phase error"* inherent in horns is reduced. This reduction in phase-error increases the aperture efficiency and also reduces the proximity correction for a given value of r. Further, if the flare-angle is reduced to zero, that is for the case of open-ended hollow waveguide, an unusually large aperture efficiency results that cannot be explained by the usual Huygens-Kirchoff antenna theory. For some frequencies within the operating band, open-ended guides (OEG) have aperture efficiencies of more than 150 percent (see section 3.1.6).

---

*The "phase-error" is the deviation from uniform-phase illumination. Antennas with uniform-phase illumination are said to be cophasal.

2.4 Some Conclusions

For most EM hazard meter calibrations it is important to be able to establish power densities of 10 mW/cm² or more, the current maximum permissible exposure level for plane-wave fields. If one wishes to establish these densities with relatively inexpensive moderate-power oscillators, he is constrained, at the present time, to approximately the following powers: 60 watts from 100 MHz to 1 GHz, 40 watts from 1 to 1.5 GHz, 25 watts from 1.5 to 2 GHz, and 20 watts from 2 to 20 GHz. Then eq. (2.12) indicates that many horn antennas are not small enough given the constraints imposed here. For example, eq. (2.12) indicates that for a 25 watt oscillator A_p should be no larger than 250 cm². For frequencies below 2.6 GHz, this is a rather small aperture, and the availability of such horns is poor or non-existent.

The above discussion, and a perusal of the commercially available horns, allows some important conclusions. Within the constraints of r > 1, moderate oscillator power, and the need to establish power density readings of 10 mW/cm²:

   (1) Most of the popular Naval Research Laboratory [15] design horns are too large.

   (2) Above 2.6 GHz (above the WR430 band) some horns with sufficiently small apertures and flare angles are available that have gains of about 15 dB or more. (The importance of this approximate gain minimum is explained below.)

   (3) From about 2.6 GHz down, available pyramidal horns are increasingly unsatisfactory due to increasing aperture area.

   (4) Because it is highly desirable that the probe being calibrated be much smaller than the aperture dimensions of the horn,* EM hazard meters with large probes are relatively difficult to calibrate.

Conclusion (2) above does not follow from eq. (2.12) for the WR284 band (2.6 to 3.95 GHz); however, a more detailed calculation for an available small flare-angle horn with about 15 dB gain (about 15 by 20 cm aperture dimensions) shows that 10 mW/cm² can be generated with less than 20 watts of power. At higher frequencies the availability of small aperture horns is better, and less than 10 watts of power are required for some available horns.

The importance of having a gain of 15 dB or more is that comparisons between measured and calculated gain values for such horns has, to date, always been within ± 0.3 dB. For horns with smaller gain values, our experience at the National Bureau of Standards (unpublished work) has been that the calculated gain values are likely to be in error by more than ± 0.3 dB. Apertures with dimensions smaller than about one wavelength have

---

*When using the proximity correction method, it is possible for the field to be significantly non-uniform over the dimensions of the probe if the probe is too large compared to the aperture of the radiator.

much larger gain values than predicted by the usual Huygen's-Kirchoff theory. (Open-ended guide has nearly twice the calculated gain at its lower frequency limit.)   Since essentially the same theory is used to calculate near-field corrections for horns, one would also expect the calculated corrections to be more accurate for horns with 15 dB or more gain.   The accuracy of near-field calculations is difficult to assess, but it is reasonable to assume uncertainty limits of 10 percent of the decibel value of the correction for r > 1 [3].   Then for r = 1, nearly all horns will have a corresponding uncertainty of less than ± 0.2 dB.

Though it would be better to use measured gain and near-zone correction values for EM hazard meter calibrations, it would appear from the last paragraph that calibration fields with near-field power densities known to well within ± 1 dB can be established above 2.6 GHz by using calculated values. It must be emphasized, however, that near-field corrections at points on the radiation axis of the horn may differ substantially from the proper proximity correction if the probe of the EM hazard meter is not much smaller than the aperture of the horn.   Most EM hazard probes are quite small, but it is probably true that not all existing EM hazard meters can be calibrated under the stated constraints without some experimentally determined proximity corrections.   Regardless of these limitations, it is obvious that the existing calibration capability above 2.6 GHz is much more satisfactory than that below 2.6 GHz.   Therefore, due to the limited funding available, it was decided to concentrate entirely on the frequency region below 2.6 GHz where satisfactory radiators with easily calculable characteristics are not available.

2.5   Open-Ended Hollow Waveguide Radiators

For frequencies below 2.6 GHz, it is tempting to use open-ended hollow waveguide (OEG) radiators to establish calibration fields for EM hazard meters. Some obvious advantages of OEG radiators are:

(1)   They are inexpensive.

(2)   They can be obtained in long lengths (important for extending the radiating aperture well in front of an absorbing wall without having a flange exposed to add to the ever-present scattering problem).

(3)   They are rugged, stable, and lightweight.

(4)   They are apparently the smallest aperture-type radiators commercially available, thus providing maximum field intensity per watt of source power.

(5)   Accurately scaled waveguides are available from the WR430 band to at least as low as the WR2300 band (0.320 to 0.490 GHz) so that gain and near-field correction values can be easily scaled.

Some other advantages of OEG radiators are:

    (6)   The gain function of OEG is smooth and nearly linear with frequency.

    (7)   For most EM hazard meters, particularly those of recent design, the proximity corrections with respect to OEG will be smooth and nearly linear with frequency.

    (8)   Along the radiation axis, at least, the backscatter from fields incident on OEG is quite small (important for reducing the interaction between the transmitting antenna and probe).

Advantage (6) is known from [11] and from the measurements reported in section 3.1; advantage (7) follows from the fact of smooth and nearly linear gain and assuming a field sensor small compared to the local field variations (i.e., small compared to the aperture of the OEG); advantage (8) was determined as part of the work reported in section 3.1.3.

In addition to the relatively small calibration field volume provided by OEG, there are two other potential disadvantages associated with the use of OEG. One of these is the fairly large reflection coefficient of OEG. As shown in table 1, WR430 has a maximum in-band $|\Gamma|$ of about 0.282 (VSWR less than 1.8) at 1.7 GHz. However, this reflection coefficient magnitude is not serious since, if not corrected by tuning, existing moderate-power sources can tolerate this degree of mismatch and the forward power loss is less than 8 percent.

The most serious potential disadvantage of OEG is its relatively low directivity. The relatively low directivity of OEG causes a strong illumination of the surrounding test chamber which then produces a relatively large amount of scatter into the test region. However, the resulting multipath interference level will not necessarily be large at the calibration point because the ratio of the separation between the aperture and the calibration point to the separation between the aperture and the scattering objects is relatively small when using small apertures. That is, the calibration point is isolated from the surrounding chamber by "dispersion" of the radiated field. Some rough calculations indicate that for the WR430 band the MPI problem will be less when using OEG in small chambers than when using a 15 dB gain horn. This assertion is consistent with the measurements reported in section 3.3.3.

It can be concluded that OEG makes a very satisfactory radiator for calibrating EM hazard meters with small field sensors when only moderate source power is available and when small test chambers are to be used. Some necessary restrictions and techniques when using OEG are discussed in section 3.3.

11

2.6 Summary of Experimental Work Performed

Regarding the discussion in the preceding sections, the experimental work was limited to that necessary to implement the use of OEG radiators for use in the WR430 band and below. Specifically, the following tasks were performed:

(1) Gain measurements for open-ended WR430 (and scaling of the results for WR650, 975 and 1500). (See section 3.1).

(2) Determining near-field corrections for small probes located on-axis in front of open-ended WR430 (and scaling the results for WR650, 975, and 1500). (See section 3.2).

(3) A calibration of an EM hazard meter was performed for the WR430 band to confirm the suitability of the calibration scheme. (See section 3.3).

3. EXPERIMENTAL WORK PERFORMED

3.1 Gain Measurements

3.1.1 Introduction

Gain measurements for WR430 guide were performed on a small indoor range using an extrapolation technique [4]. This technique permits accurate gain measurements at reduced separations and is often employed by the National Bureau of Standards to measure gain-standard horns. It is theoretically rigorous and includes provisions for evaluating both proximity and multipath interference (MPI) effects. The technique is similar to the usual two-antenna or three-antenna methods [3,4] for absolute gain measurements, but involves the measurement of the received signal as a function of separation distance. If the measurement is properly designed [3,4], the recorded data will clearly show any significant MPI as periodic variations as a function of separation. These variations are averaged out and the smoothed signal-versus-separation data is processed in a way that allows an extrapolation of the signal to "infinite" separation [4]. In the following discussion this technique is assumed to be familiar, but some further explanation is included for continuity.

Open-ended pieces of waveguide will be nearly identical in their electrical and radiating characteristics if they are within the usual specified tolerances (± 0.013 cm for both dimensions of WR430). Since the aperture efficiency will be nearly constant for small differences in the aperture dimensions, the differences in effective receiving area, and thus also the gain, will be nearly proportional to the differences in physical aperture area. For WR430 guides within specification, the gains will be within ± 0.015 dB. This small variation justifies the use of the two-antenna method for the measurements reported here.

12

Insofar as the antennas are identical, their polarizations are identical
so that any polarization mismatch is due merely to rotational misalignment.
Since the polarization patterns are broad and it is easy to accurately align
pieces of OEG, the error due to polarization mismatch can be expected to be
well within 0.01 dB. Further, due to the broad radiation pattern of OEG,
the error due to directional misalignment of the guides can be expected to
be well within 0.01 dB. Then the working formula for the gain measurement
reported here is

$$ G = M^{\frac{1}{2}} \left[\frac{4\pi d}{\lambda} \right] \left(\frac{N \, {}^{f}P_{LO}}{{}^{i}P_{L}} \right)^{\frac{1}{2}} \tag{3.1} $$

where M is a calculated mismatch factor (see section 3.1.5), d is the separa-
tion between the planes of the open ends of the guides, ${}^{i}P_{L}$ is the power
delivered to the load when the generator and load (see figure 1) are coupled
directly, ${}^{f}P_{LO}$ is the power delivered to the load through the antenna trans-
mission path and after any MPI variations are removed (see section 3.1.3), and
N is an experimentally determined correction factor for proximity effects
(see section 3.1.4).

3.1.2 Equipment Used and System Calibration

The pieces of WR430 used for the gain measurements were each about 60 cm
long and without flanges on the open-ends. The open ends and the faces of
the flanged ends were machined to provide surfaces precisely orthogonal to
the axis of the guides. The dimensions and angles of the open ends were
measured and found to be well within tolerance.

The equipment arrangement is shown in figure 1. This simple measurement
system provided adequate accuracy for measuring the insertion-loss ratio
$({}^{f}P_{L}/{}^{i}P_{L})$ as needed for the gain determination. The source was a sweep-
oscillator providing at least 20 mW of power over the WR430 band. Previous
measurements on this source showed no significant spurious frequencies in this
band except for harmonic frequencies, which are removed by the harmonic filter.
The digital frequency meter was checked against a standard frequency and found
to be within one part in 10^{6} immediately before the gain measurements. The
digital power meter was used to provide easily known changes in the trans-
mitted power. It was tested and found to be linear within 1 percent over a
20 dB dynamic range by comparing it against an NBS Type II Power Measuring
System [12] (utilizing a single-element bolometer to avoid the error associated
with dual-element bolometers). The "PIN" diode modulator and square-wave driver
were used to provide a modulated signal for the receiving system. The dc
block isolates the rest of the system from any low frequency noise produced by
the PIN diodes and also prevents ground-loop noises when the generator and load
are coupled.

13

The receiving system was designed to be small and light so that it could be easily moved to the generator for generator-load couplings. The cable between the (tunnel-diode) detector and the 1 kHz amplifier was long enough so that only the hollow-to-coax guide adapter, 20 dB pad, and detector had to be moved. The logarithmic amplifier was used to provide a more convenient output signal for recording on the X-Y recorder. The receiving system (the "load") was calibrated in terms of the X-Y recorder trace by coupling the generator and load and comparing the receiving system against an NBS Type II Power Measuring System (utilizing a single-element bolometer) that was temporarily substituted for the digital power meter. Over the same 10 dB range that would be used to record the received signal as a function of separation, the receiving system was linear to within 0.02 dB. This linearity test includes any effects due to possible changes in the modulation waveform as a function of power level.

The X-axis of the recorder was driven by a voltage proportional to the separation distance between the apertures of the antennas. This voltage was derived from a mechanically-driven potentiometer connected to the cart supporting the receiving antenna tower (see figure 2). The X-axis trace of the recorder was calibrated by using a pointer attached to the cart and measuring the separation distance by means of a measuring tape placed along one of the rails. The separation distance could be measured to within the resolution permitted by the recorder, ± 0.1 percent. Before collecting data to compute the insertion-loss-ratio versus frequency, the RF power was turned off and the load was manipulated in the same manner that would be used in these measurements while observing both the X and Y axes of the recorder. This was done to determine if significant instabilities were present due to changes in ground loop currents when the generator and load were coupled, 1 kHz noise leaking into the receiving system, etc. Instabilities from such problems were well below 0.01 dB.

3.1.3 Insertion Loss Versus Distance

Data were collected to determine the insertion-loss ratio at 11 frequencies; 100 MHz intervals from 1.6 GHz to 2.6 GHz. For each frequency, with the generator and load connected to the antennas, a "final" transmitted power level was set and the power meter reading ^fP_M was recorded. Then 6 or more recordings of the received signal were made. For each recording, the absorber blocks behind each antenna were moved to new positions along the guide, but not advancing the absorbers more than about 15 cm from the rear-most positions, so that the effects of "forward-scatter" and "backscatter" (see figure 2) could be observed. Figure 3 shows a typical set of these recordings. Most antennas have sufficiently small back-lobes in their patterns that forward-scatter and back-scatter are not important during a gain measurement (though it is always necessary in a careful measurement to evaluate these effects.)

14

For OEG, however, these scattering components are quite important, as shown
by the recorded data. Unlike the other important scattering components, the
forward-scatter and back-scatter do not change very much in electrical phase
at the receiving aperture (i.e., the path-length difference with respect to
the direct wave does not change much for these components with changes in
separation), necessitating absorber movements to induce the required phase
changes. In figure 3 the shorter variations, with periods of $\lambda/2$, in each
recording are due to "inter-antenna" (or "mutual") MPI (see figure 2) and
the offsets between the individual recordings are due to forward-scatter and
back-scatter. Other sources of MPI, such as floor scatter, are apparently
very small. The MPI effects were averaged-out* by drawing curves through
the extremities of the MPI variations and then drawing the locus of points
midway between these two curves. This final curve, $^fS_0$, can be interpreted
as the signal that would be received in the absence of scattering. Before and
after the group of 6 receiving signal curves were recorded, the generator and
load were coupled, the source power was set to give zero dB on the Y-axis,
and the "initial" power level ^iP_M of the power meter was noted. (If ^iP_M was
significantly different for the before and after readings, the data were
discarded and the insertion-loss measurement was repeated.) Then the ratio
$^fP_{LO}/^iP_L$ is easily obtained from

$$-10 \log(^fP_{LO}/^iP_L) = {}^fS_0 + 10 \log(^fP_M/^iP_M) \qquad (3.2)$$

where $^fP_{LO}$ has been used to emphasize that the MPI has been averaged-out in
this insertion-loss ratio.

Note that the $\lambda/2$ variations in figure 3 are no more than $\pm$ 0.1 dB even
at the closest separations. This indicates that open-ended guide does not have
a strong scattering component back along its axis for 2.0 GHz. Essentially
the same mutual MPI variations were obtained for the other frequencies within
the WR430 band.

For the gain calculations, the value of $^fS_0$ at 24 cm was used. (The
rest of the $^fS_0$ curve was used to determine the proximity correction as discussed
later.) The uncertainties in the insertion-loss due to the transmitting and
receiving systems (including drift, connector uncertainties, the resolution
of the recorder, and spurious frequencies) are estimated to be within $\pm$ 0.1 dB.
To this value must be added (a) the uncertainty due to the MPI from the
absorbing walls behind the absorber blocks mounted on the waveguide, and
(b) the uncertainty due to the fact that the "true" extremes of the MPI
from the absorber blocks may not have been recorded. To estimate (a), the

---

*Strictly, the MPI effects should be averaged-out from a signal proportional
to the received power rather than the log of this signal. However, for
variations of less than a few tenths of a dB, there is negligible error
associated with averaging a "logarithmic" recording rather than a "power"
recording.

absorbing walls were moved independently of the absorber blocks and the perturbations in the received signal were observed to be less than ± 0.05 dB. For (b), it is believed reasonable to assume no more than ± 0.05 dB uncertainty at 24 cm. Then the total estimated uncertainty in the insertion-loss is ± 0.2 dB for any frequency at 24 cm, and the corresponding uncertainty in the gain will be ± 0.1 dB.

3.1.4 Proximity Corrections

The proximity corrections N (section 3.1) are determined, essentially, by fitting a polynomial function to the relative received power times distance squared as the dependent variable and inverse distance as the independent variable [4]. This function is then normalized by dividing by the leading (constant) term of the series, and the result is, within the accuracy allowed by the experimental data, equal to 1/N. Usually, automatic data processing is used to perform measurements by the extrapolation technique. However, the necessary equipment was not available for this measurement, and a graphical analysis was used instead. In this instance, the loss of accuracy involved in using a graphical analysis is believed to be small.

Figure 4 shows a graphical determination of 1/N for 2.0 GHz. The eight plotted points were obtained from the relative received power after averaging out the perturbations due to multipath interference; that is, the power as determined from eq. (3.2). Following the usual practice, the separation distance is measured in terms of $r = d/(a^2/\lambda)$. Also note that a horizontal intercept has been assumed for $1/r = 0$. Extrapolation data for (strictly) cophasal apertures will show a horizontal intercept at $1/r = 0$ [13]. Though OEG radiators are not highly cophasal, due to fairly large edge effects, a horizontal intercept was assumed and allowance was made for this approximation in the error analysis. Dividing the curve of figure 4 by the intercept of 0.416 at $1/r = 0$ gives 1/N for all distances.

The relatively large forward and back-scatter involved complicates the analysis of the uncertainties for N. Referring to figure 3, the large offsets in the recorded data are due to the forward and back-scatter. However, these offsets do not have a large effect on N. For example, if the upper and lower envelopes of figure 3 are used instead of the median curve to determine N, the value of N for 24 cm separation is changed by only about ± 0.15 dB. Therefore, it is estimated that the combined uncertainty due to MPI and the assumption of a horizontal intercept (the only important sources of uncertainty in N) are no more than ± 0.2 dB for 2 GHz and 24 cm separation. However, these uncertainty limits can be reduced by the procedure discussed next.

The determinations of the proximity correction N for all the other frequencies were performed as described above. Figure 5 shows the values of N versus frequency for 24 cm separation. A "least squares" linear function has been fitted to these values. (Because the gain of OEG is very nearly linear with frequency, it is reasonable to assume that small proximity corrections for OEG will also be nearly linear with frequency.) The values of N given by the linear fit are believed to be within ± 0.1 dB, and the corresponding uncertainty in the gain is ± 0.05 dB. (Linear functions for N versus frequency determined for other distances and scaled for other waveguides are shown in table 3.)

3.1.5 Mismatch Factor

Rather than using tuners to provide matched conditions for the gain measurement, measured reflection coefficients were used to calculate the mismatch factor M in eq. (3.1). If the reflection coefficients of the transmitting and receiving antennas are identical (not necessarily true for antennas that have identical radiation characteristics), then M is given by [2]

$$
M = \left\{ \frac{|1 - \Gamma_G \Gamma_A|^2 |1 - \Gamma_A \Gamma_L|^2}{|1 - \Gamma_G \Gamma_L|^2 (1 - |\Gamma_A|^2)^2} \right\}
\tag{3.3}
$$

where Γ_G, Γ_L, and Γ_A are (respectively) the reflection coefficients of the generator, load, and OEG antennas. The use of eq. (3.3) is justified by the measurements of the reflection coefficients of the pieces of OEG (discussed below) that showed these coefficients to be very nearly identical.

All of the reflection coefficients were measured with a carefully calibrated automatic network analyzer which was recalibrated several times during these measurements. The measurements of Γ_G and Γ_L were done both before and after the insertion loss measurements. For all frequencies, the before and after measurements were in good agreement ($|\Gamma|$ within 0.005).

The measurements for each piece of OEG were repeated six times for each frequency. During these measurements, the OEG's were radiating into an anechoic chamber and pieces of absorbing material were mounted around the guides near the flange end. For the six repeated measurements of the reflection coefficients, the OEG's were moved with respect to the chamber and the absorbing collars were moved along the guides in increments over about $\lambda/2$ for the operating frequency. As expected, the measured reflection coefficients varied because of the changes in the received energy scattered back from the chamber and the absorbing collar. However, these variations were fairly small. A variation of ± 0.01 for $|\Gamma_A|$ and ± 5 degrees for θ_A were the greatest for any frequency and any scattering configuration. These maximum values were used for a conservative estimate of the uncertainty limits for the reflection coefficients. The reflection coefficients for each OEG were

17

indistinguishable, and the values listed in table 1 are the average of the measurements for both OEG's. The maximum value of $|\Gamma_A|$ at 1.7 GHz and the minimum value at 2.5 GHz were fairly repeatable for both guides and probably represent the actual variations of $|\Gamma_A|$ with frequency for the OEG's.

The values of $M^{\frac{1}{2}}$ ranged from about 1.05 to 1.1, and the maximum uncertainty in $M^{\frac{1}{2}}$, calculated from the uncertainty limits for the reflection coefficients, was ± 0.05 dB.

3.1.6 Results and Discussion

Table 2 gives the results of a least-squares linear regression for the numeric (not dB) gain versus frequency data for WR430. This table also gives the corresponding functions scaled for WR650, WR975, and WR1500. The deviation of the data points from the linear function was within ± 0.03 dB, and a quadratic fit to the data was not significantly better. The only significant uncertainties for each data point are those mentioned at the ends of sections 3.1.2, 3.1.3, and 3.1.4. The simple sum of these estimated uncertainties is ± 0.2 dB (or ± 4.7%). Though the averaging involved in the linear regression might justify somewhat lower uncertainty limits, the author prefers not to claim less than ± 0.2 dB for the gains as expressed by the functions of table 2.

Gain measurements for OEG are rare. However, some comparisons can be made to previous measurements. Newell [14] has measured a gain of 6.72 ± 0.2 dB for open-ended WR650 at 1.4 GHz. The gain formula in table 2 gives a gain of 6.92 dB. The difference between these values may be in part due to the fact that Newell's measurement was for an OEG with hollow-to-coaxial guide adapter. FitzGerrell [11] has measured the gain of open-ended WR90. This waveguide does not have the 2:1 ratio of inside dimensions characteristic of the waveguides listed in table 2; therefore, only an approximate comparison can be made with his results. Using the ratio between the large dimensions of the guides for scaling, the formulas of table 2 give gain values roughly 0.1 dB higher than FitzGerrell's results.

The gain of OEG is considerably larger than predicted by existing theoretical calculations. The results of various calculations differ but usually give values of about 2.0 for WR430 at 1.6 GHz. For example, [5] yields a value of 1.9, which is much less than the value of 3.71 given by the formula in table 2. Also interesting is the fact that OEG has an aperture efficiency greater than 1. The aperture efficiency of WR430 at 1.6 GHz is 1.74, that is the effective receiving area is 1.74 times greater than the physical aperture area.

3.2 Near-Field Corrections

Except in the approximate sense mentioned in the next paragraph, the desired on-axis near-field correction for a radiating antenna cannot be determined from the proximity correction N for power transfer between two identical

18

antennas. The usual procedure for measuring the near-field correction is to use a small receiving probe moved along the axis of the antenna of interest. Then the response of the probe is processed in the same manner as for the measurement of the proximity correction for N during a gain measurement (see section 3.1.4). Actually, this procedure gives the proximity correction for power transfer from the antenna to the probe. This proximity correction will be nearly equal to the near-field correction for the antenna provided (a) that the near-field configuration does not differ significantly from the far-field configuration (a reasonable assumption for r > 1) and (b) that the probe has an antenna or field sensor that is much smaller than the aperture of the antenna of interest. For the near-field measurements of WR430 OEG reported here, a small dipole-diode field sensor was moved along the radiation axis of the guide. These measurements were difficult to make because of the poor quality of the existing NBS anechoic chamber. The high MPI level in the NBS chamber limited the accuracy of the measurements, though the accuracy is satisfactory with respect to ± 1 dB EM hazard meter calibrations.

As noted in previous work [1], the (decibel) near-field correction 10 Log C for the usual horn antenna at moderately near distances is approximately equal to 5 log N, where N is for the case of the power transfer between two identical horns. Because the calculation of proximity corrections is based on essentially the same theory as gain calculations and gain calculations for OEG are inaccurate, it is by no means certain that this approximation will hold for OEG. However, within the accuracy of the near-field measurements performed as part of the work reported here, the approximation seems to hold for OEG. For example, the near-field correction measurement for WR430 at 20 cm and 2.6 GHz was 0.33 ± .15 dB, which compares fairly well with the value of 0.41 dB for 5 Log N calculated from the formula of table 3. Measurements of the near-field correction were made at several other frequencies and these values also were within about ± 0.1 dB of 5 Log N. Thus, until better near-field correction measurements can be performed for OEG, 5 Log N (where N is given by table 3) is believed to provide essentially the best values available for the near-field corrections. The agreement between the measured values for 10 Log C and 5 Log N will justify uncertainty limits of only about ± 40% of the decibel correction.

3.3 Applying the Results

3.3.1 Summary of the Calibration Method

Though the gain and near-field measurements for open-ended guide and other radiators are difficult, it is easy to use the results for calibrating EM hazard meters. Employing open-ended guides below 2.6 GHz, a small anechoic chamber with dimensions about 10 meters long and 5 meters in height and width should allow calibrations from above 20 GHz down to 500 MHz (if premium quality

19

absorbing material for use down to 500 MHz is used to line the chamber). The field sensor to be calibrated is placed on-axis in front of the radiator at a near field distance of, roughly, 1 to 2 a^2/λ and the near-field power density S_n is calculated from the net power accepted by the antenna, the gain of the antenna, and the near-field correction:

$$S_n = \left(\frac{G}{C}\right)\left(\frac{P}{4\pi d^2}\right) . \qquad (3.4)$$

(See discussion in 2.2 concerning "near-field gain.")

Gain values for some commonly available horns are given in [15], near-field corrections for these horns are given in [1], and near-field gain values can be easily calculated for any pyramidal horns using the technique described in [6]. For open-ended waveguide, tables 4 through 7 in this report give the net power ("forward minus reflected") required to establish a 10 mW/cm^2 field level for various frequencies at two near-field distances for WR430, WR650, WR975, and WR1500. Note that more than 60 watts of net power are required for frequencies below 0.9 GHz. For frequencies below 0.9 GHz, the following proce-dure can be used to calibrate at the 10 mW/cm^2 level: (a) calibrate the meter at a lower level, say 5 mW/cm^2, at one of the distances given in tables 6 or 7; (b) move the probe to a closer position on-axis so that a reading of 10 mW/cm^2 or a little more can be obtained; (c) adjust the input power to achieve precisely the same reading on the instrument that was recorded for the 5 mW/cm^2 level field and note the net transmitted power; (d) multiply this net power by 2 (or by 10 divided by the particular mW/cm^2 field level used in (a)) and increase the net power to this amount; (e) the reading on the meter should now be the same as would be obtained at the original probe position if sufficient source power were available to establish a 10 mW/cm^2 level at that distance. If the probe is too large this procedure may not be valid due to the difficulties described in section 2.2. However, it is believed there are presently no EM hazard probes that are so large as to invalidate this procedure for WR975 waveguides and larger. Though definitive information is lacking, it seems very unlikely that a field sensor with largest dimension smaller than $1/4\,\lambda$ would be too large. In effect, the procedure (a) through (e) extends the near zone calibration method to closer distances where the near-field correc-tion is apt to be substantially different for various probes (unless they are all very small).

Some important precautions are given in the next section. With reasonable care, and given an adequate anechoic chamber, the techniques described here will allow EM hazard meter calibrations using OEG to within about ± 0.7 dB total uncertainty limits. This estimate is for the simple sum of the following: ± 0.2 dB for the gain uncertainty, ± 0.1 dB for the near-field correction at the low end of the frequency band and ± 0.15 dB at the high end of the band; ± 0.2 dB for the measurement of the net power; ± 0.2 dB for multipath inter-ference at the low end of the band and ± 0.15 dB at the high end of the band.

20

These error estimates are about the same as for horn antennas used at 2.6 GHz in a small anechoic chamber.

3.3.2 Precautions and Suggestions

(1) The choice of absorbing material for the anechoic chamber is very important. For a small chamber one wishes to use the minimum necessary absorber thickness since the absorber thickness can seriously limit the working volume of the lined chamber. For a 10 m by 5 m by 5 m chamber for use above 500 MHz the best choice is believed to be the solid-pyramidal-foam type with about 61 to 66 cm thickness (24 to 26 inches).

(2) The blocks of absorber mounted on the OEG's in figure 2 were used to aid in analyzing the scattering during the OEG gain measurements. They should not be used during EM hazard meter calibrations since they would neces-sarily be closer to the aperture of the guide than the absorbing wall behind the aperture and would thus likely increase the forward scatter.

(3) The radiator used for the calibration should extend well in front of the absorbing wall to minimize the forward scatter. This is particularly important for OEG radiators. A good practice is to extend the aperture in front of the wall at least three times the absorber thickness.

(4) The estimate of uncertainties for MPI mentioned at the end of the last section are based on the observed MPI for isotropic probes placed in front of OEG at the distances listed in tables 4 through 7. For directive probes oriented for maximum response, the MPI level will be no greater than this and should be much less. However, if polarization or response patterns are recorded for directive probes, fairly large errors could occur for some parts of these patterns. The problems involved in making accurate polarization or response patterns for EM hazard meters is beyond the scope of this report.

(5) Often the floor of the chamber will scatter more than the ceiling or walls because of equipment and walkways located on the floor. Orienting the E-planes of OEG or horns horizontally will help reduce the floor scatter by means of the (usually) sharper H-plane patterns of these radiators.

(6) As mentioned in sections 1, 2, it is considered desirable to minimize the interaction between the sensor and the rest of the meter during EM hazard meter calibrations. Using horizontal polarization helps to achieve this condition since it is then relatively easy to orient any instrument cables orthogonal to the electric vector of the field.

(7) Particularly when using OEG radiators, the equipment used for the calibra-
    tion may suffer from interference at the source frequency. The meter being
    calibrated may also be so susceptible to interference that a valid cali-
    bration cannot be obtained (in which case the meter is useless at that
    frequency).

(8) Determining the net power by subtracting the measured reverse power from
    the measured forward power could possibly cause a significant error due
    to scattering back to the radiator from the chamber or from the probe
    being calibrated. The energy scattered back to the radiator will, in part,
    be received by the radiator and erroneously appear to be part of the wave-
    guide reflected power. For the scattering from a reasonably good anechoic
    chamber, the resulting error is small. These errors were evaluated with
    respect to a rather poor chamber during the OEG reflection coefficient
    measurements (see section 3.1.5) and found to cause changes in the apparent
    $|\Gamma|$ for the OEG of only ± 0.01. Most EM hazard probes also cause small
    scattering. However, good practice requires that a new type of probe that
    has not been previously investigated should be moved along the axis of
    the radiator to induce perturbations in the reflected power. These perturba-
    tions are a direct measure of the errors resulting from the scattering
    from the probe (unless they are averaged out as a part of the calibration
    procedure).

3.3.3   Test Calibrations

A small isotropic probe was available for the following tests. This probe
was calibrated at 2.5 GHz both with WR430 OEG (at 20 cm) and with a "15 dB"
gain WR284 horn whose gain was known from previous measurements. The two
calibrations agreed to within 0.2 dB, well within the ± 0.5 dB uncertainty
estimate for the calibration using the horn. These measurements were made in
a chamber with dimensions of only about 5 m by 2.5 m by 2.5 m.

During the calibration with WR430 OEG, the MPI was measured by moving the
probe along the OEG axis and by moving the absorbing wall behind the OEG.
The total MPI was less than ± 0.2 dB throughout the band. For comparison,
a "15 dB" gain WR430 horn was substituted for the OEG and the MPI was found to
be somewhat larger, ± 0.25 dB, for an equivalent separation in terms of a^2/λ.
(These measurements tend to confirm the discussion at the end of section 2.5.)
For the lower frequency horns, there will likely be considerably more advan-
tage in using OEG rather than horns.

22

4. REFERENCES

[1] Bowman, Ronald R. and William E. Jessen, Calibration techniques for RAMCOR densiometer antennas, NBS report (unpublished),

[2] Bowman, R.R., Near-zone calibrations for antennas and field intensity meters, Rome Air Development Center Technical Report No. RADC-TR-69-415 (January 1970).

[3] Bowman, R.R., Field strength above 1 GHz: Measurement procedures for standard antennas, Proc. IEEE, 55, 981-990 (June 1967).

[4] Newell, Allen C., Ramon C. Baird and Paul F. Wacker, Accurate measurement of antenna gain and polarization at reduced distances by an extrapolation technique, IEEE Trans. on Antennas and Propagation, AP-21, No. 4, 418-431 (July 1973).

[5] Chu, L.J., Calculation of the radiation properties of hollow pipes and horns, Journal of Applied Physics, 11, 603-610 (Sept. 1940).

[6] Jull, E.V., Finite-range gain of sectoral and pyramidal horns, Electronics Letters, 6, No. 21, 680-681 (October 15, 1970).

[7] IEEE Test Procedures for Antennas, No. 149 (Revision of IRE 2S2) (January 1965), IEEE Trans. on Antennas and Propagation, AP-13, 437-466 (May 1965).

[8] Crawford, M.L., Generation of standard EM fields for calibration of power density meters 20 kHz to 1000 MHz, NBSIR 75-804 (January 1975).

[9] Baird, R.C., Methods of calibrating microwave hazard meters, Biologic Effects and Health Hazards of Microwave Radiation, Proc. of an Intl. Symposium Warsaw, 228-236 (October 1973).

[10] Soejima, T., Fresnel gain of aperture aerials, Proc. IEE (London), 110, 1021-1027 (June 1963).

[11] FitzGerrell, R.G., Swept-frequency antenna gain measurements, IEEE Trans. on Antennas and Propagation, AP-14, 173-178 (March 1966).

[12] Larsen, N.T. and F.R. Clague, The NBS Type II Power Measurement System, 1970 ISA Annual Conf. Proc., Philadelphia, PA, Paper No. 712-70, 25, Pt. 3, 12 pages (Oct. 1970).

[13] Wacker, P.F., Electromagnetics Division, National Bureau of Standards, Boulder, Colorado, Private Communication.

[14] Newell, A.C., Electromagnetics Division, National Bureau of Standards, Boulder, Colorado, Private Communication.

[15] Slayton, W.T., Design and calibration of microwave antenna gain standards, Naval Research Lab., Washington, D.C., Rept. 4433 (Nov. 1954).

Table 1. Measured reflection coefficients of WR430 open-
ended guide, 58.8 ± 0.1 cm long.

Frequency	$\lvert \Gamma_A \rvert$	θ_A
(GHz) (±0.0001)	(Dimensionless) (±0.01)	(Degrees) (±5)
1.6	.262	-165.0
1.7	.282	-56.6
1.8	.279	73.4
1.9	.265	-136.5
2.0	.266	23.8
2.1	.245	-167.9
2.2	.248	8.2
2.3	.232	-172.6
2.4	.223	11.6
2.5	.207	-156.9
2.6	.214	31.1

Table 2. Gain formulas for various waveguides.

Waveguide	Gain Formula
WR430	$G_{430} = -0.054 + 2.353\ F$
WR650	$G_{650} = -0.054 + 3.557\ F$
WR975	$G_{975} = -0.054 + 5.335\ F$
WR1500	$G_{1500} = -0.054 + 8.208\ F$

Notes: The formulas are for numeric gain (not dB). The
frequency F is in units of GHz.

Table 3. Proximity corrections for various waveguides.

WR 430

d(cm)	Formula
20	N = 1.0072 + 0.0764 F
24	N = 1.0028 + 0.0499 F
28	N = 0.9896 + 0.0392 F
32	N = 0.9967 + 0.0256 F

WR 650

d(cm)	Formula
30	N = 1.0072 + 0.1155 F
36	N = 1.0028 + 0.0754 F
42	N = 0.9896 + 0.0593 F
48	N = 0.9967 + 0.0387 F

WR 975

d(cm)	Formula
45	N = 1.0072 + 0.1732 F
54	N = 1.0028 + 0.1131 F
63	N = 0.9896 + 0.0889 F
72	N = 0.9967 + 0.0580 F

WR 1500

d(cm)	Formula
70	N = 1.0072 + 0.2665 F
84	N = 1.0028 + 0.1741 F
98	N = 0.9896 + 0.1367 F
112	N = 0.9967 + 0.0893 F

25

Table 4. Net power P_{10} required to establish 10 mW/cm^2 at two distances on-axis in front of open-ended WR 430 waveguide. Also shown are the (numeric) gain G, near-field reduction 1/C, and the near-field gain G/C.

R = 20 CM

Frequency (GHz)	P_{10} (Watts)	G	1/C	G/C
1.60	14.40	3.71	0.94	3.49
1.70	13.58	3.95	0.94	3.70
1.80	12.86	4.18	0.93	3.91
1.90	12.22	4.42	0.93	4.11
2.00	11.64	4.65	0.93	4.32
2.10	11.11	4.89	0.93	4.52
2.20	10.64	5.12	0.92	4.73
2.30	10.20	5.36	0.92	4.93
2.40	9.81	5.59	0.92	5.13
2.50	9.44	5.83	0.91	5.32
2.60	9.10	6.06	0.91	5.52

R = 24 CM

Frequency (GHz)	P_{10} (Watts)	G	1/C	G/C
1.60	20.30	3.71	0.96	3.57
1.70	19.13	3.95	0.96	3.78
1.80	18.09	4.18	0.96	4.00
1.90	17.17	4.42	0.95	4.22
2.00	16.34	4.65	0.95	4.43
2.10	15.59	4.89	0.95	4.64
2.20	14.90	5.12	0.95	4.86
2.30	14.28	5.36	0.95	5.07
2.40	13.71	5.59	0.94	5.28
2.50	13.19	5.83	0.94	5.49
2.60	12.70	6.06	0.94	5.70

Table 5. Net power P_{10} required to establish 10 mW/cm^2 at two distances on-axis in front of open-ended WR 650 waveguide. Also shown are the (numeric) gain G, near-field reduction 1/C, and the near-field gain G/C.

R = 30 CM

Frequency (GHz)	P_{10} (Watts)	G	1/C	G/C
1.00	34.21	3.50	0.94	3.31
1.10	31.21	3.86	0.94	3.62
1.20	28.72	4.21	0.93	3.94
1.30	26.62	4.57	0.93	4.25
1.40	24.82	4.93	0.92	4.56
1.50	23.26	5.28	0.92	4.86
1.60	21.90	5.64	0.92	5.16
1.70	20.70	5.99	0.91	5.46
1.80	19.64	6.35	0.91	5.76

R = 36 CM

Frequency (GHz)	P_{10} (Watts)	G	1/C	G/C
1.00	48.28	3.50	0.96	3.37
1.10	43.98	3.86	0.96	3.70
1.20	40.41	4.21	0.96	4.03
1.30	37.39	4.57	0.95	4.36
1.40	34.81	4.93	0.95	4.68
1.50	32.58	5.28	0.95	5.00
1.60	30.62	5.64	0.94	5.32
1.70	28.90	5.99	0.94	5.63
1.80	27.37	6.35	0.94	5.95

Table 6.   Net power P_{10} required to establish 10 mW/cm^2 at two distances on-axis
            in front of open-ended WR 975 waveguide. Also shown are the (numeric)
            gain G, near-field reduction 1/C, and the near-field gain G/C.

R = 45 CM

Frequency (GHz)	P_{10} (Watts)	G	1/C	G/C
0.70	73.45	3.68	0.94	3.46
0.75	68.74	3.95	0.94	3.70
0.80	64.64	4.21	0.93	3.94
0.85	61.02	4.48	0.93	4.17
0.90	57.81	4.75	0.93	4.40
0.95	54.93	5.01	0.92	4.63
1.00	52.35	5.28	0.92	4.86
1.05	50.02	5.55	0.92	5.09
1.10	47.90	5.81	0.91	5.31
1.15	45.96	6.08	0.91	5.54
1.20	44.19	6.35	0.91	5.76

R = 54 CM

Frequency (GHz)	P_{10} (Watts)	G	1/C	G/C
0.70	103.56	3.68	0.96	3.54
0.75	96.81	3.95	0.96	3.78
0.80	90.92	4.21	0.96	4.03
0.85	85.73	4.48	0.95	4.27
0.90	81.12	4.75	0.95	4.52
0.95	77.00	5.01	0.95	4.76
1.00	73.30	5.28	0.95	5.00
1.05	69.95	5.55	0.94	5.24
1.10	66.91	5.81	0.94	5.48
1.15	64.13	6.08	0.94	5.71
1.20	61.59	6.35	0.94	5.95

Table 7. Net power P_{10} required to establish 10 mW/cm^2 at two distances on-axis in front of open-ended WR 1500 waveguide. Also shown are the (numeric) gain G, near-field reduction 1/C, and the near-field gain G/C.

R = 70 CM

Frequency (GHz)	P_{10} (Watts)	G	1/C	G/C
0.45	179.61	3.64	0.94	3.43
0.50	162.36	4.05	0.94	3.79
0.55	148.28	4.46	0.93	4.15
0.60	136.57	4.87	0.93	4.51
0.65	126.68	5.28	0.92	4.86
0.70	118.20	5.69	0.92	5.21
0.75	110.87	6.10	0.91	5.55

R = 84 CM

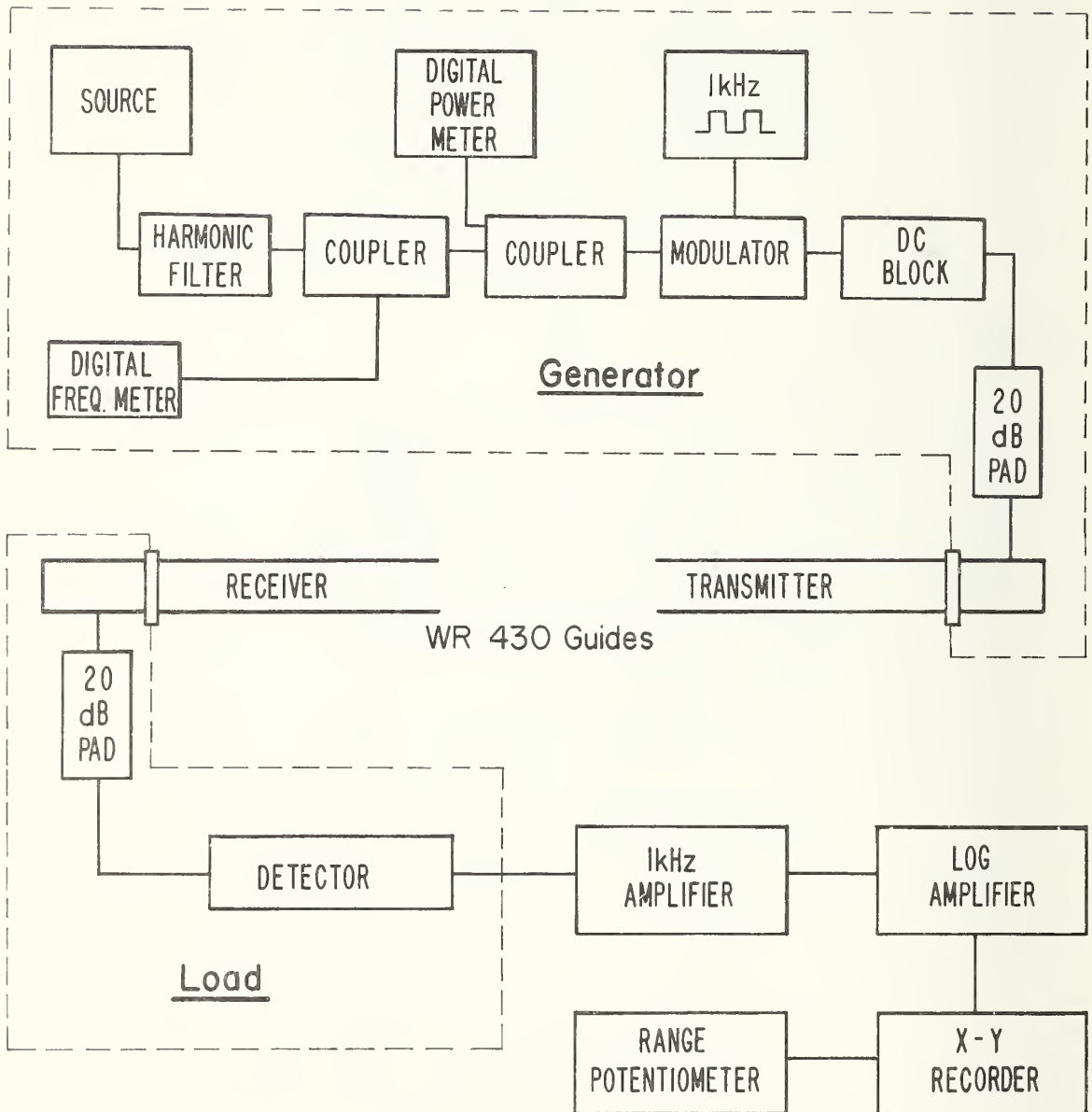| Frequency (GHz)	P_{10} (Watts)	G	1/C	G/C
0.45	253.31	3.64	0.96	3.50
0.50	228.56	4.05	0.96	3.88
0.55	208.36	4.46	0.95	4.26
0.60	191.55	4.87	0.95	4.63
0.65	177.36	5.28	0.95	5.00
0.70	165.21	5.69	0.94	5.37
0.75	154.70	6.10	0.94	5.73

Figure 1. Block diagram of equipment used for the measurement of the gain of open-ended WR430 waveguide.
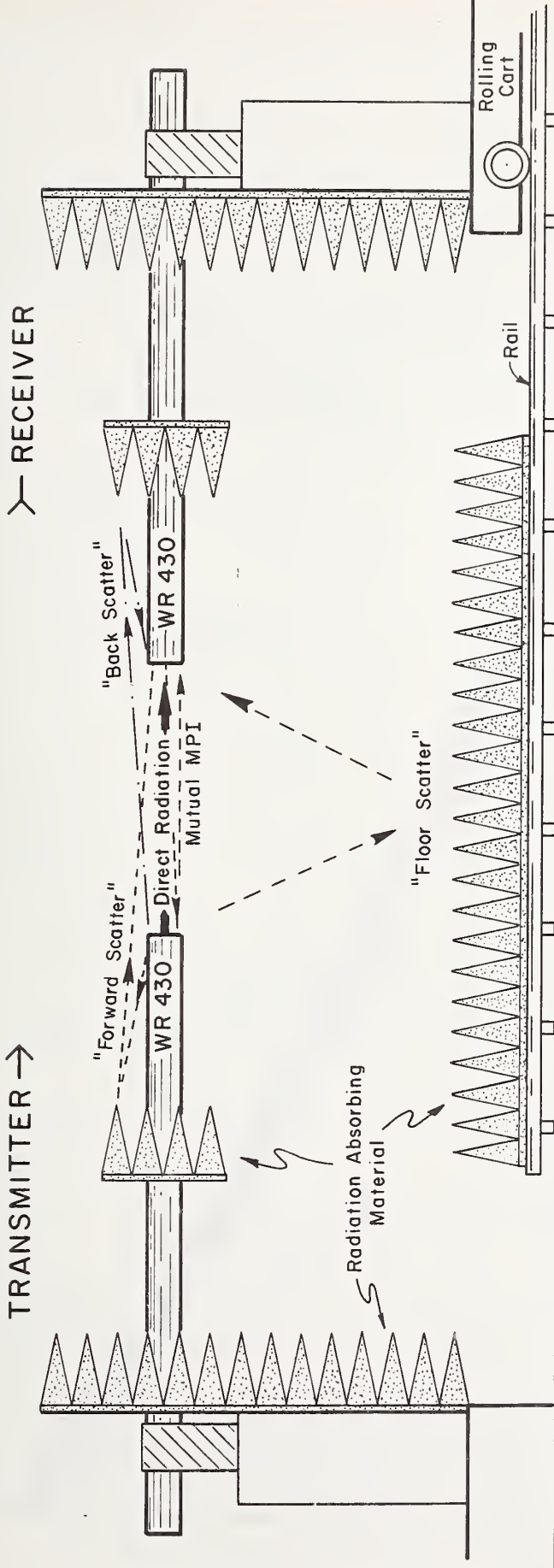
Figure 2. Antenna range configuration showing the important sources of scattering. The walls and ceiling were also covered with radiation absorbing material.
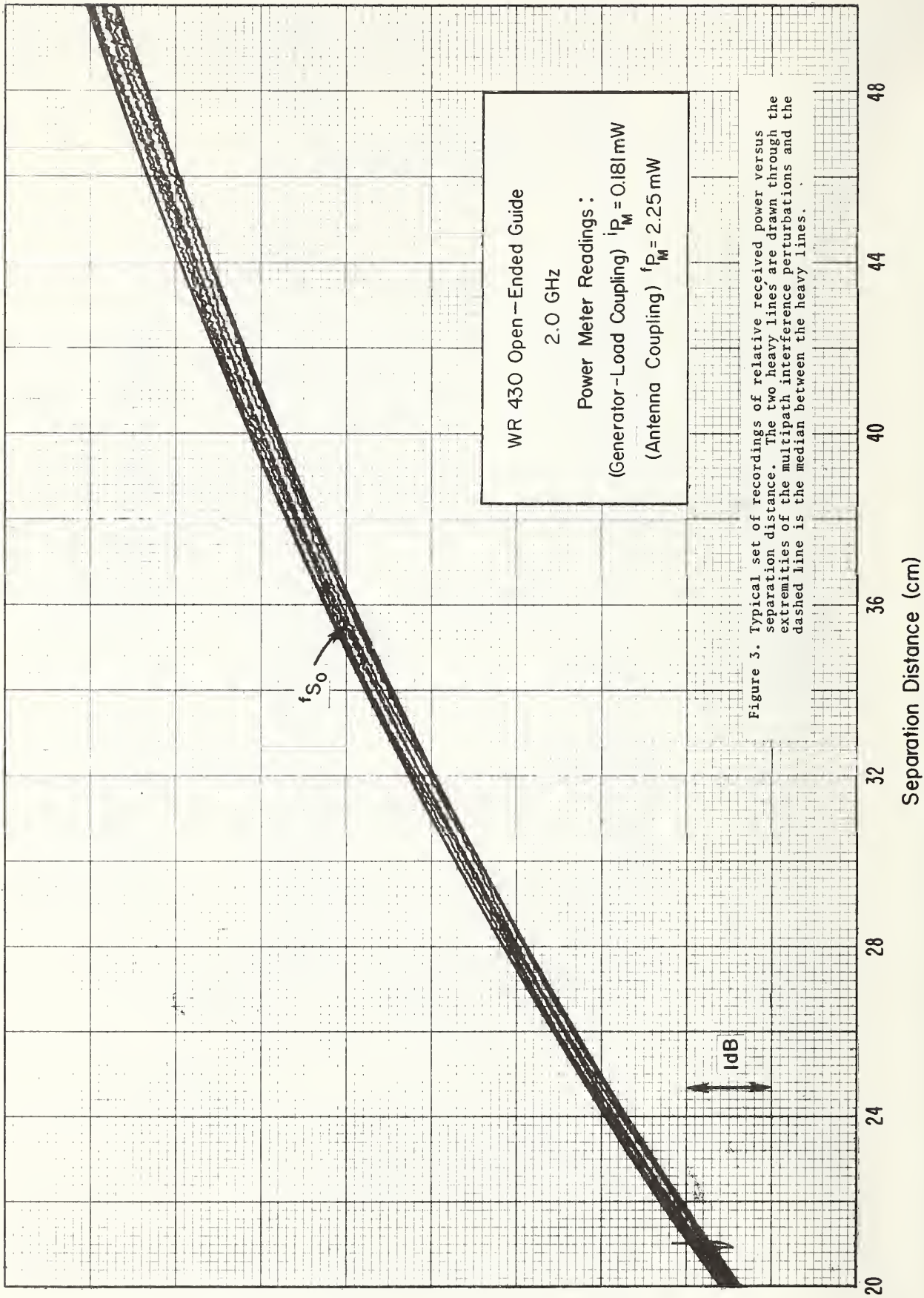
Figure 3. Typical set of recordings of relative received power versus separation distance. The two heavy lines are drawn through the extremities of the multipath interference perturbations and the dashed line is the median between the heavy lines.
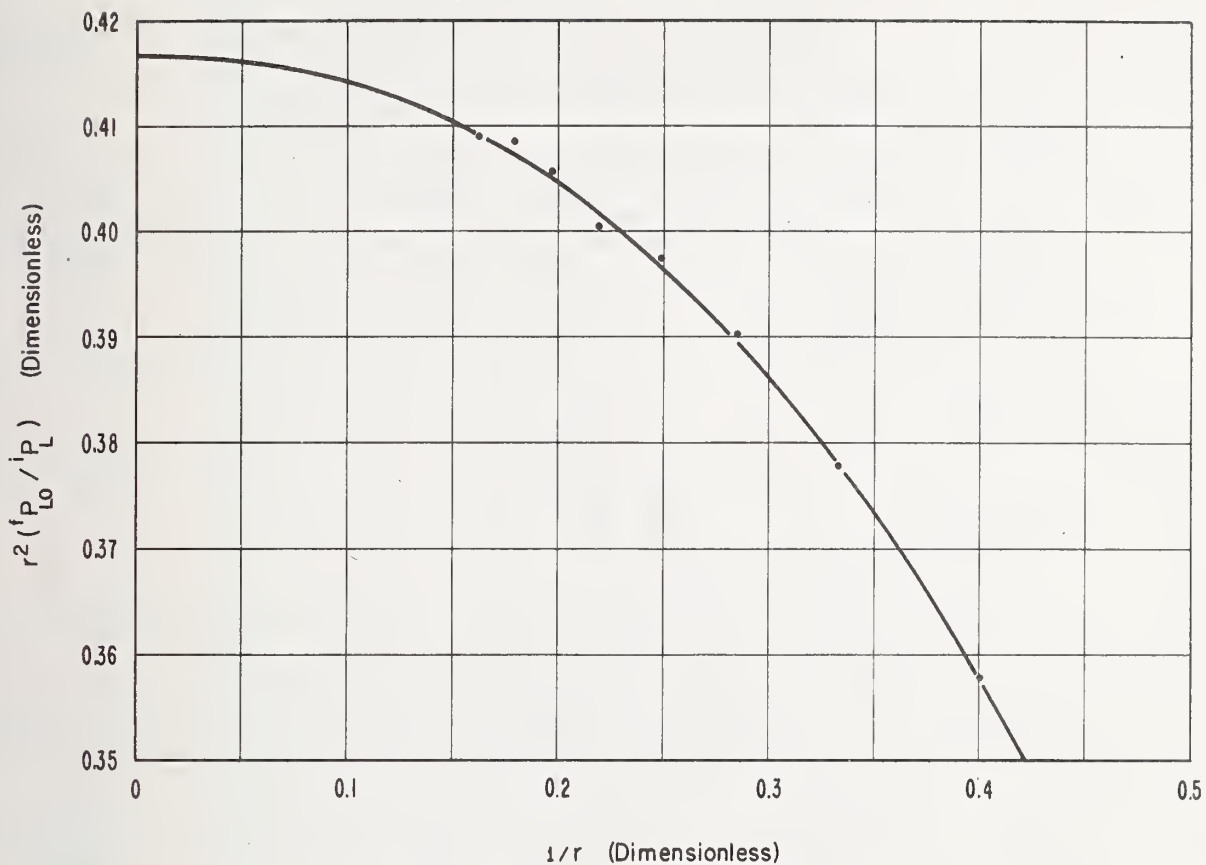
WR 430 Open-Ended Guide

2.0 GHz

Power Meter Readings:

(Generator-Load Coupling) $^iP_M = 0.181$ mW

(Antenna Coupling) $^fP_M = 2.25$ mW

Separation Distance (cm)

Relative Received Power (dB)

$^fS_0$

1 dB

32

Figure 4. Graphical determination of 1/N. The values of 1/N
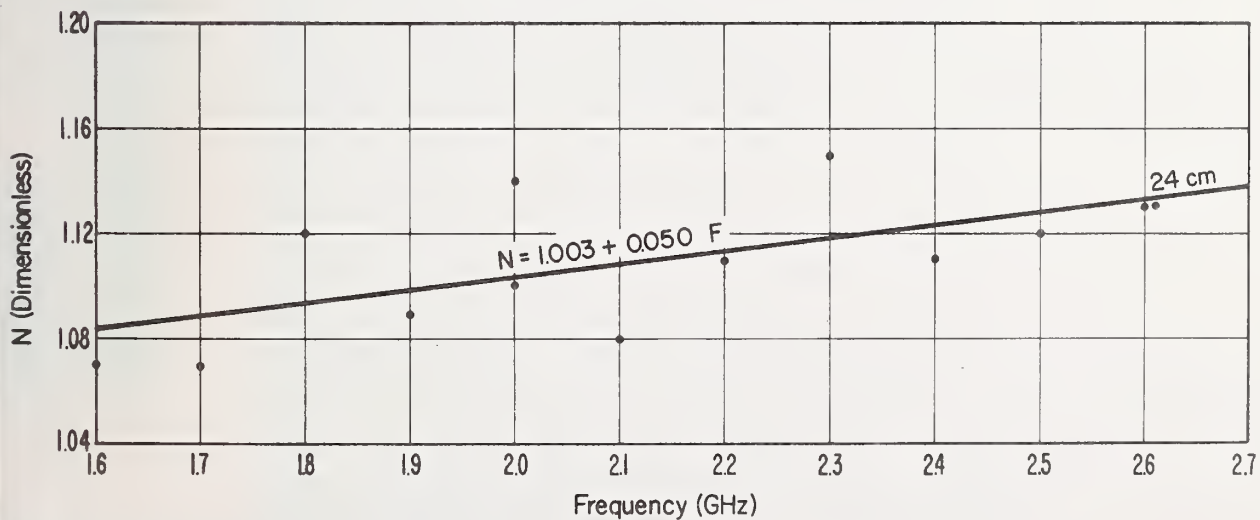are obtained by dividing the ordinates of the curve
by the intercept at 1/r = 0.

Figure 5. N versus frequency for 24 cm separation.

U.S. DEPT. OF COMM. BIBLIOGRAPHIC DATA SHEET	1. PUBLICATION OR REPORT NO. NBSIR 75-805	2. Gov't Accession No.	3. Recipient's Accession No.

4. TITLE AND SUBTITLE	5. Publication Date
Calibration Techniques for Electromagnetic Hazard Meters; 500 MHz to 20 GHz	April 1976
	6. Performing Organization Code 276.05

7. AUTHOR(S) Ronald R. Bowman	8. Performing Organ. Report No.

9. PERFORMING ORGANIZATION NAME AND ADDRESS	10. Project/Task/Work Unit No. 2765279
NATIONAL BUREAU OF STANDARDS DEPARTMENT OF COMMERCE WASHINGTON, D.C. 20234	11. Contract/Grant No.

12. Sponsoring Organization Name and Complete Address (Street, City, State, ZIP)	13. Type of Report & Period Covered
Calibration Coordination Group Army/Navy/Air Force	
	14. Sponsoring Agency Code

15. SUPPLEMENTARY NOTES

16. ABSTRACT (A 200-word or less factual summary of most significant information. If document includes a significant bibliography or literature survey, mention it here.)

The calibration techniques discussed are suitable for producing fields for calibrating most electromagnetic (EM) hazard meters to within ± 1.0 dB using a minimum of laboratory space and oscillator power. Above about 2.6 GHz, adequate equipment and standards have been available for these calibrations. Below this frequency the large apertures of the usual horn radiators require more power than is available from medium power oscillators. Further, calibrations in closed systems are difficult except at frequencies well below 1 GHz. Thus there is a need for small-aperture gain standards from about 500 MHz to 2.6 GHz. The main portion of the work reported here consists of accurate gain measurements for open-ended hollow waveguide radiators (OEG) for use from 500 MHz to 2.6 GHz. Other characteristics of this type of radiator important for EM hazard meter calibration were also determined: near-field corrections, reflection coefficients, and aperture scattering. The suitability of the calibration scheme was tested by performing calibrations at 2 GHz on an EM hazard meter with both a horn radiator and an OEG radiator.

17. KEY WORDS (six to twelve entries; alphabetical order; capitalize only the first letter of the first key word unless a proper name; separated by semicolons)

Calibrations; electromagnetic hazards; field meters; gain; microwave; near-field.

18. AVAILABILITY ☒ Unlimited	19. SECURITY CLASS (THIS REPORT)	21. NO. OF PAGES
☐ For Official Distribution. Do Not Release to NTIS	UNCLASSIFIED	37
☐ Order From Sup. of Doc., U.S. Government Printing Office Washington, D.C. 20402, SD Cat. No. C13	20. SECURITY CLASS (THIS PAGE)	22. Price
☒ Order From National Technical Information Service (NTIS) Springfield, Virginia 22151	UNCLASSIFIED	$3.75

USCOMM - ERL   USCOMM-DC 29042-P74